

THE PADME EXPERIMENT

F. Bossi, B. Buonomo, E. Capitolo (Tec.), C. Capoccia (Tec.),
S. Ceravolo (Tec.), G. Corradi (Tec.), R. De Sangro, D. Domenici, G. Finocchiaro,
L.G. Foggetta, G.S. Georgiev (Ass.), A. Ghigo, F. Giacchino (AdR), P. Gianotti (Resp.),
V. Kozhuharov (Ass.), B. Liberti, M. Martini (Ass.), A. Saputi (Tec.), I. Sarra (Ass.), B. Sciascia,
T. Spadaro, E. Spiriti, C. Taruggi (Dott.), E. Vilucchi

1 Introduction

One of the most intriguing mysteries in physics today, is that the matter seen in the universe accounts only for about 5% of the observed gravity. This has triggered the idea that enormous amounts of invisible dark matter should be present.

Among the different theoretical models that try to define what dark matter could be, there are those postulating the existence of a “Hidden Sector” populated by new particles that do not couple with those of the Standard Model (SM). The connection within these two worlds is theoretically realized by a low-mass spin-1 particle, indicated with the symbol A' , that would manifest a gauge coupling of electroweak strength to dark matter, and a much smaller coupling to the SM hypercharge ¹⁾. This Dark Photon (DP) could be the portal connecting ordinary and dark worlds.

The PADME experiment aims to search for signals of such a DP studying the reaction:

$$e^+e^- \rightarrow \gamma A'$$

using the positron beam of the LNF LINAC and identifying the A' as a missing mass signal.

PADME (Positron Annihilation into Dark Matter Experiment) is an international collaboration of about 50 people that involves, in addition to LNF researchers, scientists from the INFN sections of Roma1, Roma2 and Lecce, the Sapienza and Tor Vergata Universities of Rome (IT), the Salento University (IT), the Sofia University (BG), the Cornell University (USA), and the Atomki Institute of Debrecen (H).

The apparatus, built, installed and commissioned with the beam in 2018, in 2020 had a second data acquisition period (from July to December 2020). The first part was dedicated to beam tuning and detectors calibration, while from September $\sim 5 \times 10^{12}$ positrons on target (POT) were recorded to start addressing the main physics goal.

2 The PADME experiment

The goal of the PADME experiment is to search for DPs produced in the annihilation process of the positron beam of the LNF LINAC with a thin diamond target and then identified using a missing mass technique ²⁾.

Figure 1 shows a scheme of the apparatus whose basic elements are:

- a low divergence positron beam, impinging on a thin, active target, capable of monitoring the beam size and intensity;
- a vacuum chamber to avoid spurious particle interactions;

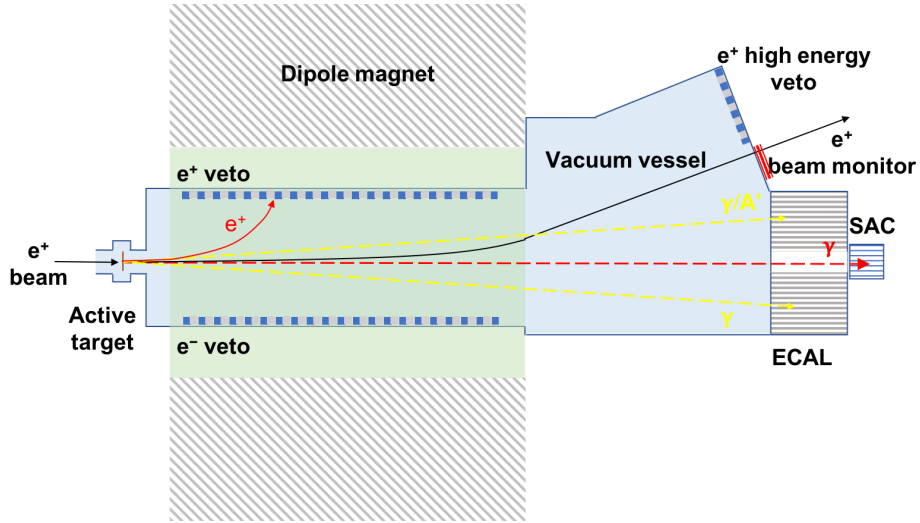


Figure 1: *The layout of the PADME experiment From left to right: the active target, the positron/electron vetoes inside the magnetic field, the high energy e^+ veto near the non-interacting beam exit, the e.m. calorimeters (ECal, SAC), the solid state beam monitor detector.*

- a magnet to deflect the beam of positrons emerging from the target, with the additional task of allowing the measurement of the momentum of the interacting positrons, thus contributing to the rejection of the Bremsstrahlung background;
- a finely-segmented, high-resolution e.m. calorimeter, with the main duty to measure the momentum of the single SM photons (ECal).

Since the processes that mainly take place in the beam-target interaction are Bremsstrahlung and $e^+e^- \rightarrow \gamma\gamma(\gamma)$, to cut out these background events, two extra components are crucial:

- a fast Small Angle Calorimeter (SAC), placed behind the central hole of the primary one. This is used to detect and veto background photons (mainly from Bremsstrahlung);
- three stations of plastic scintillator slabs, located inside the vacuum chamber, two within the dipole magnet gap (Pveto and Eveto), and the third one on the beam exit (HEPveto), to veto charged particles produced in the interaction.

To have a more accurate monitoring of the beam, in the target region are installed two planes of silicon pixel detectors placed up and down stream the active diamond target. Each plane consists of two MIMOSA 28 Ultimate chips, developed for the upgrade of the STAR vertex detector³⁾. These devices integrate a Monolithic Active Pixel Sensor (MAPS) with a fast binary readout. Each sensor consists of a matrix of 928×960 pixels of $20.7 \mu\text{m}$ side with a thickness of $50 \mu\text{m}$. For the STAR experiment the chips, that dissipate $150 \text{ mW}/\text{cm}^2$, operate in air without cooling. For PADME, the detector has been placed in vacuum and a modified PCB has been developed by the LNF electronic service to provide cooling.

The MIMOSA detector cannot stay on the beam line during the data taking, therefore an extra monitoring device is placed out of the vacuum on the positron beam exit trajectory. This is an array (6×2) of Timepix3 chips⁴⁾ able to record either the time-of-arrival (ToA) and the energy of the incident particles providing excellent energy and time resolutions. A single silicon

chip is designed in 130 nm CMOS technology and contains 256×256 pixels ($55 \times 55 \mu\text{m}^2$). This detector has been built and installed at LNF by the ADVACAM company ⁵).

The physics potential of the PADME experiment extends beyond DP search. The built detector is also sensitive to any new light particle, including scalars and pseudo-scalars, that are produced in the positron-on-target interaction. An estimate of the physics potential of PADME to search for axion like particles as well as other exotic states is ongoing thanks to a strong synergy with the LNF theoretical division. In addition, it will be possible to perform measurements of the differential cross sections for Bremsstrahlung emission for positrons in the $O(100 \text{ MeV})$ energy range and to address the multi-photon annihilation cross sections.

3 Activity of the PADME LNF Group

The starting of 2020 saw the PADME collaboration stuck for the pandemic that has hit the planet, with an unavoidable slowing down of all the activities. The analysis of the data set collected from Oct. 2018 to Feb. 2019 provided the calibrations of each detector component and the definition of the best beam conditions for the physical data taking. These required a change in the beam line in order to reduce the high level of beam-induced background that was observed during the first PADME Run.

The PADME experiment uses the positron beam coming from the BTF line 1 that since October 2018 is exclusively dedicated to the experiment. Positrons are accelerated up to 550 MeV after being generated in the LINAC on a W-Re converter of $2 X_0$ (Positron converter) located after the first electron accelerating sections (primary positron beam) or are produced by a primary electron beam of 750 MeV hitting a Cu converter of selectable X_0 (1.7, 2, or 2.3) (BTF target) located before a 1 m thick concrete wall that separates the LINAC from the BTF experimental hall (secondary positron beam). An energy selection system, and some collimators on the BTF transfer-line, define momentum, spot size, and intensity of the beam. Figure 2 shows the layout of the PADME beam line.

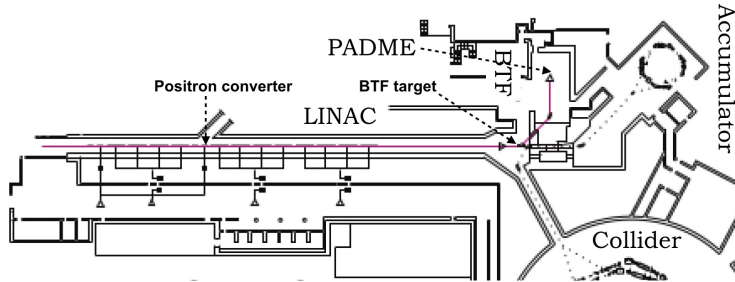


Figure 2: *Layout of the PADME beam line.*

The majority of the data collected during the PADME commissioning run were acquired with the positrons produced at the BTF target and only few days, at the end of February 2019, were instead collected with the primary positron beam. This second data set turned out to be more clean and therefore, it was decided to adopt this setup for the physics data taking, even if it costs a small reduction to the maximum energy available for the experiment. Furthermore, another source of beam-induced background was identified in the Be window ($500 \mu\text{m}$ thick) that separated the accelerator vacuum from the experiment one. This diaphragm was located just before the last dipole that bends the positrons onto the PADME target. When the particles traversed this material, they lost energy and therefore, when they entered in the dipole, were not

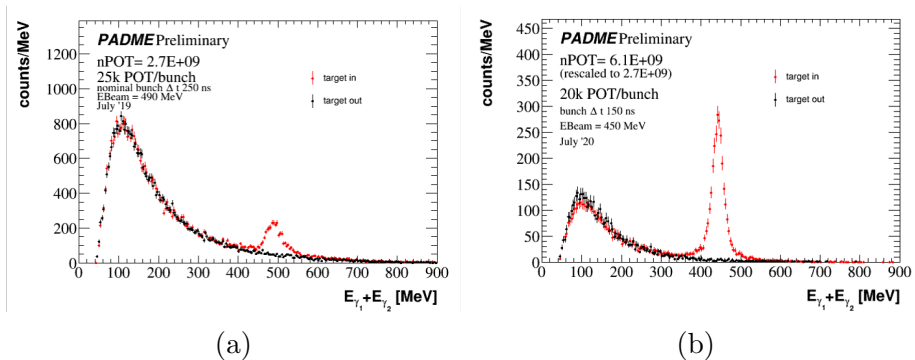


Figure 3: *Invariant mass of 2-photon final state. Red histogram corresponds to the data collected with the target on-beam, the black one represents the background and it has been collected with the target off-beam. a) 2019 beam setup b) 2020 beam setup (details on the beam settings are indicated in the figures).*

perfectly driven. They hit the magnet iron, or other supports, creating showers that finally reach the PADME calorimeters. To overcome this problem, it was decided to move this window more upstream in the beam line, closer to the BTF target, behind the tick LINAC wall. The material used, was also changed (Mylar) and reduced in thickness ($145 \mu\text{m}$). These changes to the beam line were taking place starting from March 2020 in order to restart PADME beam commissioning in July.

4 The PADME Data Taking

Just after the national lockdown imposed by the pandemic, the staff of BTF and of the LNF vacuum service made the necessary changes to the BTF line 1 and starting from beginning of July, PADME could restart the beam studies. Up to the summer break, different beam configurations were tested in order to define the best bunch length and beam multiplicity. The maximum energy available was slightly lower (450 MeV) due to a fault in the C-modulator of the LINAC. At the end of these operations, it was achieved a beam condition allowing to reduce, more than three times, the level of background on the calorimeters. Figure 3 shows the invariant mass of two-photon final states measured with the primary beam setup of July 2019 and with that of July 2020. In 2019, the beam energy was 490 MeV, the bunch length 250 ns and the particle multiplicity was $\sim 25\text{k}/\text{bunch}$. In 2020 the positron energy was 450 MeV, the bunch length 150 ns and the multiplicity $\sim 20\text{k}/\text{bunch}$. The red histogram represents the invariant mass of true 2-photon final states, while the black one is obtained making the same requirements on the detector signals, but without the target on the beam line. Therefore, this represents the beam-induced background of the measurement. Comparing the plots resulting from 2019 data taking (fig. 2a)) with those collected in 2020 (fig. 2b)), the background reduction is striking evident.

Starting from September the 15th, the PADME data taking entered in the phase of acquisition for physics analysis. Up to the beginning of December $\sim 5 \times 10^{12}$ POT were recorded on tape.

5 List of Conference Talks presented by LNF Speakers in Year 2020

Here below, it is the list of conference presentations given by LNF PADME members:

1. P. Gianotti, “The physics program of the PADME experiment”, invited talk at the Excited

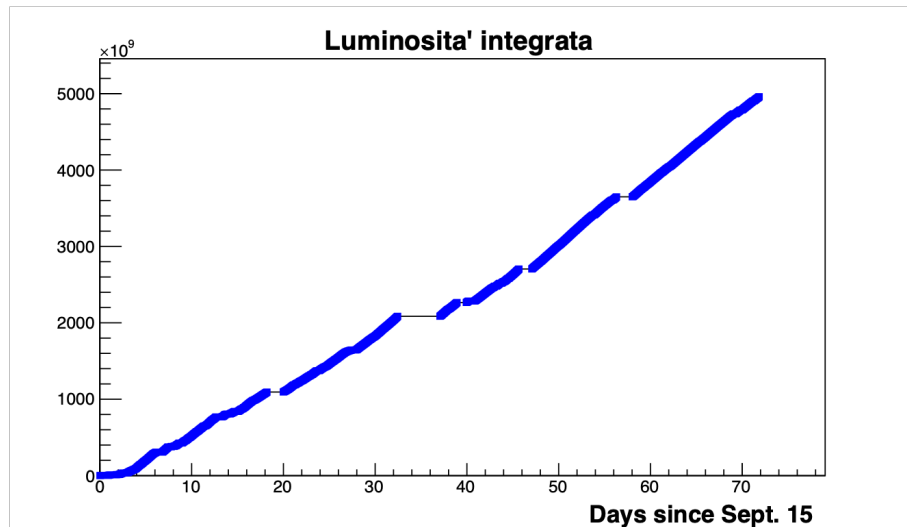


Figure 4: *PADME* integrated luminosity in 2020 data taking.

QCD 2020 Conference, Krynica Zdroj, 3 - 7 Feb. 2020.

2. F. Giacchino, "Searching for light dark matter portals", online seminar, 6 Feb. 2020.
3. D. Domenici, "The PADME detector at LNF", talk at the International Conference Instrumentation for Colliding Beam Physics (INSTR-20), Novosibirsk, 24 - 28 Feb. 2020.
4. C. Taruggi, "The Padme detector", talk at the 9th International Conference on New Frontiers in Physics (ICNFP 2020), Crete, 4 Sep. 2 Oct. 2020.
5. B. Sciascia, "L"esperimento PADME", plenary talk at the Congresso Nazionale Società Italiana di Fisica, 14 - 18 Sep. 2020.

For the complete list of presentations to conferences given by the PADME collaborators, refer to <http://padme.lnf.infn.it/list-of-papers/>.

6 List of Publications by LNF Authors in Year 2020

Here below, it is the list of papers published by PADME LNF members in 2019:

1. P. Albicocco *et al.*, "Characterisation and performance of the PADME electromagnetic calorimeter", *JINST* **15** (2020) no.10, T10003.
doi:10.1088/1748-0221/15/10/T10003.
2. P. Gianotti, "The Physics Program of the PADME Experiment", *Acta Phys. Polon. Supp.* **14** (2021), 35.
doi:10.5506/APhysPolBSupp.14.35.

The complete list of papers published by the PADME collaboration in 2019 can be find here <http://padme.lnf.infn.it/papers/>.

References

1. B. Holdom, Phys. Lett. B 166, 196 (1986).
M. Pospelov, Phys. Rev. D 80, 095002 (2009).
2. M. Raggi and V. Kozhuharov, Rivista del Nuovo Cimento 38 no. 10, (2015).
DOI 10.1393/ncr/i2015-10117-9
3. I. Valin *et al.*, JINST 7, C01102 (2012).
4. T. Poikela *et al.*, JINST 9, C05013 (2014).
5. ADVACAM s.r.o., U Pergamenky 12, 17000 Praha 7, Czech Republic, (<https://advacam.com>).